Techno-economic assessment of pervaporation desalination of hypersaline water

by Indah Prihatiningtyas

Submission date: 17-Mar-2022 01:08PM (UTC+0700)
Submission ID: 1786180316
File name: tekno_ekonomi.pdf (2.68M)
Word count: 8092
Character count: 41808

Desalination 527 (2022) 115538

Contents lists available at ScienceDirect

Desalination

journal homepage: www.elsevier.com/locate/desal

Techno-economic assessment of pervaporation desalination of hypersaline water

Indah Prihatiningtyas [a,b,*], Al-Hasan Ammar Hussien Al-Kebsi [c], Yusak Hartanto [d], Tsegahun Mekonnen Zewdie [a,e], Bart Van der Bruggen [a,f,**]

[a] Department of Chemical Engineering, KU Leuven, Celestijnenlaan 200F, B-3001 Leuven, Belgium
[b] Department of Chemical Engineering, Mulawarman University, Jalan Sambaliung No.9, Sempaja Selatan, Samarinda, Kalimantan Timur, Indonesia
[c] Ecole Nationale Superieure des Industries Chimiques, Universite de Lorraine, rue Grandville 1, BP 20451, 5400 Nancy, France
[d] Materials and Process Engineering (iMMC-IMAP), UC Louvain, Place Sainte Barbe 2, 1348 Louvain-la-Neuve, Belgium
[e] Bahir Dar University, Faculty of Chemical and Food Engineering, Department of Chemical Engineering, Bahir Dar, Ethiopia
[f] Faculty of Engineering and the Built Environment, Tshwane University of Technology, Private Bag X680, Pretoria 0001, South Africa

HIGHLIGHTS

- Techno-Economic Assessment of pervaporation desalination of hypersaline water is performed.
- The water cost increases by around 13% when the feed concentration increases from 90 g L^{-1} to 200 g L^{-1}.
- The series configuration shows the lowest thermal energy compared to the single and parallel configuration.
- PV desalination is attractive by integrating with low-grade waste heat from industrial plants as thermal energy resource.

ARTICLE INFO

Keywords:
Pervaporation
Desalination
Hypersaline water
Energy requirement
Economic analysis

ABSTRACT

The development of pervaporation desalination has seen continuous interest due to the ability of this technology to handle high salinity feeds in the absence of high hydraulic pressure. As pervaporation utilizes the difference of partial vapor pressure as the main driving force for separation, an elevated feed temperature is often needed, and this significantly increases the energy requirements of pervaporation desalination. The advancement of high-performance pervaporation desalination membranes with high water flux and salt rejection in recent years could make this desalination technology competitive to other hypersaline desalination processes. Unfortunately, there is a lack of understanding of the energy requirements necessary for an economic assessment of pervaporation desalination applied for highly saline feed solutions. In this study, the energy requirements and the economic feasibility of pervaporation desalination for hypersaline desalination were evaluated using previously developed high-performance cellulose triacetate/cellulose nanocrystals nanocomposite membranes as the membrane model. The results showed that thermal energy was still the main factor that determined the overall water production cost. Increasing the plant capacity decreased the water cost while increasing the feed salinity from 90 to 200 g L^{-1} increased the water production cost due to the drop of the water production rate, which requires to expand the membrane surface area to obtain the same plant capacity. A series configuration showed the lowest thermal energy compared to a single and parallel configuration. However, the single configuration is more attractive than a series and parallel configuration when the pervaporation desalination utilized free low-grade waste heat. Hence, PV desalination for treating hypersaline water can be competitive if the process could be integrated with low-grade waste heat from industrial plants as a thermal energy source.

* Correspondence to: I. Prihatiningtyas, Department of Chemical Engineering, Mulawarman University, Jalan Sambaliung No.9, Sempaja Selatan, Samarinda, Kalimantan Timur, Indonesia.
** Correspondence to: B. V. der Bruggen, Faculty of Engineering and the Built Environment, Tshwane University of Technology, Private Bag X680, Pretoria 0001, South Africa.
E-mail addresses: indah.ft@ft.unmul.ac.id (I. Prihatiningtyas), bart.vanderbruggen@kuleuven.be (B. Van der Bruggen).

https://doi.org/10.1016/j.desal.2021.115538
Received 19 December 2021; Accepted 27 December 2021
Available online 28 January 2022
0011-9164/© 2022 Elsevier B.V. All rights reserved.

1. Introduction

Seawater is an abundant water resource in the world. Unfortunately, this saline water cannot be directly used for human consumption. Desalination has to be used to provide fresh water from salty water sources, such as seawater or brackish water. As such, desalination has the potential to provide a breakthrough to overcome the water scarcity issues in the world. It is an attractive technology to provide fresh water, as evidenced by the growth of research on desalination, which was approximately more than 373,000 articles published for desalination from 1980 until 2021 (scholargoogle.com, using the search keyword "Desalination"). Furthermore, it has been reported that there are 15,906 operational desalination plants with a total capacity of approximately 34.81 billion m^3/year [1]. Desalination technology is constantly evolving, recently pervaporation has been interesting for desalination application and around 21,100 articles published from 1980 until 2021 (scholargoogle.com, using the search keyword "Pervaporation Desalination").

However, the increase in desalination plants brings a new problem with brine as a by-product, creating a critical environmental issue. Brine has a high salinity and has a negative environmental effect on the aquatic environment, groundwater, and soil quality [2]. Hence, the desalination brine has to be treated to minimize the disposal of brine and obtain freshwater, possibly combined with salt production. Hypersaline water becomes an environmental concern because it is not only a waste product of desalination plants but is also produced by the oil and gas industry, the waste stream of the zero-liquid discharge process, landfill leachate and wastewater of flue gas desulfurization [3].

Both membrane-based and thermal-based water purification techniques have been used for water desalination applications. The most common thermal-based water purification techniques are multi-stage flash distillation (MSF), multi-effect distillation (MED), vapor compression (VC). This conventional water purification method is energy-intensive, which utilizes high-grade energy like gas, electricity, oil, and fossil fuels, low efficiency, and high environmental impact, in addition, their complexity and different related operational problems. These shortcomings have forced researchers to search for advanced alternative technologies. One of these alternative technologies is membrane-based water purification technology (reverse osmosis (RO), electrodialysis (ED), pervaporation, and membrane distillation (MD)) which has a strong ability to be coupled with solar energy or low-grade waste heat [4]. Compared to thermal-based desalination techniques, membrane-based desalination techniques have many advantages, such as low cost, small footprint, high efficiency, and ease of operation.

Thermal desalination is the common process for desalinating highly concentrated brines. Membrane desalination processes such as ED and MD have recently been applied for treating hypersaline water [5]. Lately, some studies have highlighted the potential of pervaporation (PV) for desalination. PV allows to address the drawbacks of membrane desalination for high salinity water, such as fouling and scaling issues [6,7]. Moreover, PV has been reported to have a good performance for treating hypersaline water with NaCl concentration above 35 g L^{-1} [8–15]. Membrane distillation and pervaporation are both membrane-based water purification techniques that represent an emerging and promising technology for desalination and water/wastewater treatments application. Those technologies can be coupled with renewable energy systems (solar energy, wind energy, geothermal energy, and hydroelectric power) or low-grade waste heat for economical and energy-efficient desalination and water/wastewater treatments. Membrane distillation is a combination of thermal driven distillation and membrane separation process driven by a vapor pressure difference due to a temperature gradient across a hydrophobic microporous membrane [16]. Pervaporation is one of the effective membrane-based separation processes driven by the chemical potential gradient between the feed side and permeate side of the membrane. Pervaporation uses dense or molecular sieving hydrophilic membranes [7].

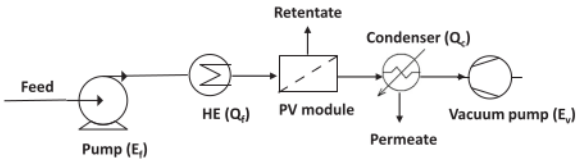

Fig. 2.1. Flow diagram of a single configuration of pervaporation desalination.

Generally, the performance of pervaporation depends on the membrane properties, the operating conditions, and the module design. Hence, there are studies available focusing on the development of PV desalination membranes and operating conditions [17–19]. Furthermore, Xie et al. [20] investigated the energy required for PV desalination. The energy requirements are important because they affect the overall process economics. Low-grade waste heat sources and heat recovery could be utilized as an energy source, and recover the heat in the condenser. Hence, the process energy requirements could be reduced, so that it might be comparable to thermal desalination technologies [20]. It is important to make desalination technologies less expensive to treat hypersaline water in view of reducing environmental damage in a cost-effective way.

The parameters needed to compare desalination processes are the energy requirements, the water production cost, technology growth trends, and environmental impact [21]. Studies related to the economic analysis of pervaporation for desalination are still lacking, particularly for hypersaline feed streams. The available economic studies are for the desalination of seawater. Previous studies reported that the cost of seawater desalination using multi-stage flash (MSF) is 1.4 $/$m^3$ [22], for multiple-effect distillation (MED) it is 1 $/$m^3$ [22,23], for vapor compression (VC) it is 0.7 $/$m^3$ [24], for reverse osmosis (RO) 0.5 $/$m^3$ [25], and for membrane distillation (MD) estimates range from 0.5 to more than 15 $/$m^3$ [26,27]. The desalination costs are different because the cost is depending on the process used and the scale of production. The cost of desalination with various desalination technologies differs largely because the cost is depending on different parameters such as feed concentration, output water quality, plant capacity and location, energy source and labor/operational costs, type of contract, political and environmental restrictions.

Furthermore, it was reported that integrating MD with industrial waste heat has the perspective to improve the economic viability. A small pilot of MD with a water production of 3.38 m^3 day^{-1} (feed rate of 92.67 m^3 day^{-1}) had a calculated cost of 0.7 $/$m^3$ with the assumption that the thermal energy requirements are fulfilled by using industrial waste heat [28].

In this work, a techno-economic assessment (TEA) at the early stage of the PV desalination process for the hypersaline feed stream is made by estimating the water cost. The experimentally determined pervaporation desalination performance, different scenarios as process models, the CAPCOST program, and cost data available in the literature were used to estimate the cost of the equipment, and the best engineering practices are integrated to develop the TEA model. In this study, there are various uncertain parameters used for estimating the water cost. Hence, a sensitivity analysis is used to investigate technical and economic parameters that have a major effect on the TEA results. Different configurations are also explored to obtain the optimal design PV desalination configuration. The impact of purchasing energy and/or integrating waste heat from the industry as free energy cost in the pervaporation desalination process on the total water cost is investigated.

2. Pervaporation desalination system

A flow diagram of pervaporation desalination is shown in Fig. 2.1 The PV process uses a heat exchanger (HE), a pump, a condenser, and a vacuum pump as basic equipment.

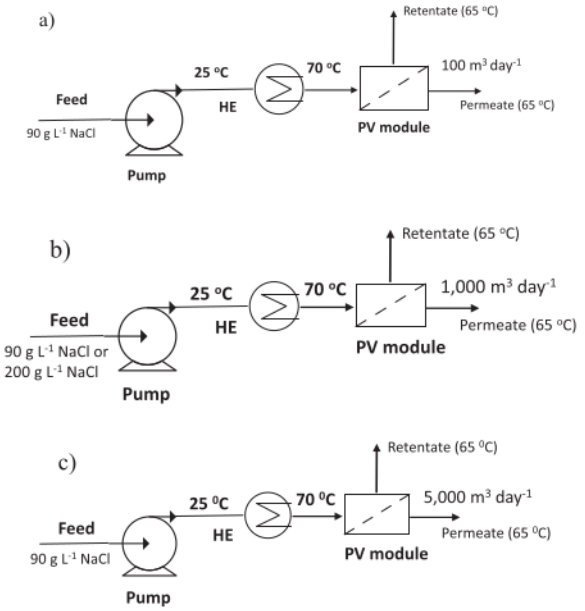

Fig. 2.2. Single stage PV desalination with different plant capacities. (a) 100 m^3 day^{-1}, (b) 1000 m^3 day^{-1}, and (c) 5000 m^3 day^{-1}.

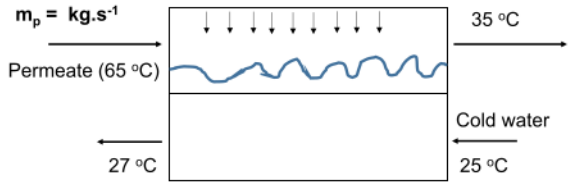

Fig. 2.3. Illustration of heat transfer in the cooling system.

The PV desalination process requires energy to increase the temperature of the feed water to reach the operating temperature and to condense the water vapor, hence the thermal energy is significant. In pervaporation, the energy requirement is categorized by the thermal energy used for feed heating (Q_f) and permeate cooling (Q_c), and the electrical energy required for the feed pump (E_f) and vacuum pump (E_v). The high energy demand involved in the PV desalination process can be reduced by using low-grade or waste heat for heating the feed or adopting a heat recovery system [20]. This aspect may be crucial for the viability of PV for desalination. Hence, a waste heat motivated PV setup was designed and analyzed in order to fulfill the energy requirements of the PV system in an efficient and a cost-effective way.

2.1. Case study

In order to carry out the techno-economic assessment (TEA) of a PV desalination for treating hypersaline water, the TEA model is developed at different capacities of a desalination plant with size Small (S) and M (Medium) [29] for four scenarios: 1) a feed stream with concentration 90 g L^{-1} of NaCl at a plant capacity of 100, 1000 and 5000 m^3 day^{-1} and a plant with a feed stream of 200 g L^{-1} of NaCl at a capacity of 1000 m^3 day^{-1}. Fig. 2.2 presents the single stage of the PV desalination at different plant capacities.

Thermal energy is used to increase the feed temperature to meet the operating temperature. In this study, PV desalination is integrated with waste heat, blast furnace gas produced by steel manufacturing plants as a waste heat source (free cost energy) with the aim to be used to heat the feed stream. Blast furnace gas has a constant flow and high recoverable potential. Blast furnace gas has a temperature ranging from 398 to 600 °C and a recoverable potential of 1.98×10^{11} MJ $year^{-1}$ [30].

In the cooling water system, the first term corresponds to the condensation of water vapor at 65 °C under vacuum and the second term corresponds to the cooling of permeate. Once the permeate is in its liquid state to a temperature of 35 °C using cold water at 25 °C, the cooling water will be discharged to the environment at a temperature of 27 °C. This is illustrated in Fig. 2.3.

In this work, the heat exchanger area, membrane area, energy required for pump, and vacuum pump were determined based on the performance of CTA/CNCs nanocomposite membranes on a laboratory scale. The feed flow rate was 75 L h^{-1} and the operating temperature was 70 °C, the water flux was 107.5 kg m^{-2} h^{-1} and 58.5 kg m^{-2} h^{-1} for a feed stream with NaCl concentration of 90 and 200 g L^{-1}, respectively [13]. To upscale the pervaporation desalination system, the feed cross-flow velocity is calculated by the Reynolds number (*Re*) approach.

$$R_e = \frac{\rho V D_h}{\mu} \tag{1.1}$$

where V is the channel average cross-flow velocity, ρ is solution density, D_h is the hydraulic diameter, and μ is the solution viscosity [31]. ρ is determined with a pycnometer, while μ is calculated based on the salinity and temperature [31,32].

Based on experimental data obtained in the laboratory, the Reynolds number was 897, which represents a laminar flow (see supporting information). In this study, the suggested scenarios for the pervaporation desalination system (Fig. 2.2) were investigated by assuming a laminar flow regime Reynolds number ranging from 897 to 2000. Similarly, Wang et al. studied the performance of a hybrid organic-ceramic

Table 2.1
Equations and assumptions for the economic calculation.

Description	Equation and assumption
Eq. 2.1. Amortization factor (a)	$a = \frac{i(1+i)^n}{(1+i)^n - 1}$ The interest rate (i) = 5%, the plant life (n) = 20 years [33,34].
Eq. 2.2. Annual capital cost (A_{CC}; $/year)	$A_{CC} = a \cdot (D_{CC} + I_{CC})$, [34].
Eq. 2.3. Direct capital cost (D_{CC}; $)	$D_{CC} = C_P + C_{HE} + C_M + C_{VP} + C_{inst}$ C_P = pump cost, C_{HE} = heat exchanger cost. C_M = membrane cost, C_{VP} = vacuum pump cost. C_{inst} = installation cost. C_{inst} = 25% of the purchased equipment costs [33].
Eq. 2.4. Indirect capital cost (I_{CC}; $)	$I_{CC} = 0.1 D_{CC}$ [35].
Eq. 2.5. Annual Operating and maintenance cost ($A_{O\&M}$; $/year)	$A_{O\&M} = A_{elec} + A_{labor} + A_{M.\,rep} + A_{maint}$, [34,36].
Eq. 2.6. Annual electricity cost (A_{elec}; $/year)	$A_{elec} = c \cdot w \cdot f \cdot m \cdot 365$, [36]. c = electric cost, 0.09 $/kWh [35,36]. w = electric power consumption (kWh m^{-3}) f = plant availability (0.9) [35,36]. m = plant capacity (m^3 day^{-1})
Eq. 2.7. Annual labor cost (A_{labor}; $/year)	$A_{labor} = \gamma \cdot f \cdot m \cdot 365$, [35,36]. γ = specific cost of operating labor, 0.05 $/$m^3$ [34,36].
Eq. 2.8. Annual membrane replacement cost ($A_{M.rep}$; $/year)	$A_{M.\,rep} = M_R \cdot C_m$ Membrane replacement rate (M_R) is 20% per year for treating high salinity water [35,37].
Eq. 2.9. Annual maintenance cost (A_{maint}; $/year)	$A_{maint} = p \cdot m \cdot f \cdot 365$ p is specific maintenance and spare parts cost = 0.033 $/$m^3$ [34,36,38].
Eq. 2.10. Total annual cost (A_{tot}; $/year)	$A_{tot} = A_{CC} + A_{O\&M}$, [34,36].
Eq. 2.11. Unit product cost (A_{unit}; $/$m^3$)	$A_{unit} = \frac{A_{tot}}{f \cdot m \cdot 365}$, [33,34,36].

hydrophilic pervaporation membrane and used Reynolds numbers ranging from 300 to ~4800 [31]. A sensitivity analysis was carried out to analyze the effect of changing the variables on the water cost. Then the impact of purchasing energy and/or integrating waste heat from the industry as free energy cost on the water cost of pervaporation desalination was also investigated. Furthermore, parallel and series configurations of PV desalination were explored to achieve the optimal water cost.

3. Methodology

3.1. Total water cost of pervaporation

In view of a techno-economic assessment (TEA) of PV desalination for hypersaline water, the water cost was estimated as a unit production cost. The calculation to evaluate the cost was taken from the literature [31–36] and modified to be fitting for pervaporation desalination. The unit cost of fresh water is defined as the total annual cost (A_{Tot}) divided by the yearly total amount of produced fresh water of pervaporation desalination [33]. The total annual cost (A_{Tot}) is determined as the sum of the annual capital cost (A_{CC}), which involves the direct capital cost (D_{CC}), indirect capital cost (I_{CC}), and annual operating and maintenance cost $A_{O\&M}$. The direct capital cost (D_{CC}) consists of the purchase of equipment (circulating pump, membrane, heat exchanger, and vacuum pump). The indirect capital cost (I_{CC}) represents the contingency cost. The equations and several assumptions made for the economic analysis are presented in Table 2.1.

3.1.1. Membrane cost

The total required area of the PV membranes is determined using the plant capacity and the calculation shown in Eq. (2.12).

$$A_t = \frac{C_{plant}}{J_p} \tag{2.12}$$

where A_t is the total membrane area (m^2), C_{plant} is the plant capacity to produce fresh water (L h^{-1}), and J_p is the permeate flux (L m^{-2} h^{-1}).

The membrane cost for desalination was reported to range from 60 to 216 \$/m^2 [28,33,39,40], while Banat and Jwaied reported that the membrane cost for a desalination plant capacity of 500 L day^{-1} was 216 \$/m^2 including the membrane cost and the PV module for laboratory scale [33]. Therefore, in this study, the membrane cost is assumed to be 140 \$/m^2 for plate and frame modules.

3.1.2. Heat exchanger cost

In the heating system, the thermal power requirement (Q_f) for operating the PV desalination system can be determined by a heat balance as follows [41]:

$$Q_f = \sum \dot{m}\, C_{ps} \Delta T \tag{2.13}$$

where $\dot{m}$ is the mass flow rate of saline water passing through heat recovery exchangers (kg s^{-1}), C_{ps} represents the heat capacity of saline water (3993 J kg^{-1} K^{-1}) [42], ΔT is the temperature difference between saline water streams across heat recovery exchangers (°C).

In the cooling system, the thermal energy required to condensate the water vapor (Q_c) is determined with Eqs. (2.14) and (2.15).

$$Q_c = m_p \lambda \tag{2.14}$$

where m_p is the mass flow rate (kg s^{-1}), and λ represents latent heat of condensation of water vapor (J kg^{-1}). Thus, the mass flow rate of water for cooling ($q_{cooling}$) is calculated as follows:

$$q_{cooling} = \frac{m_c\, C_p \Delta T_1 + m_c\, \lambda}{C_p \Delta T_2} \tag{2.15}$$

where m_c represents the flow rate from the plant capacity (kg s^{-1}), ΔT_1 is the variation of the temperature of the hot fluid, and ΔT_2 is the variation of the temperature of the cold fluid (°C). λ is 2250 kJ kg^{-1} and C_p represents the heat capacity of water (4180 J $kg^{-1}C^{-1}$).

Table 2.2
Purchase cost based on the capacity of the vacuum pump [46].

Capacity/m^3/min	Purchased equipment cost (\$)
0.11	4100
0.28	6400
0.57	8900
0.76	11,500
1.14	16,200
1.51	20,800
1.89	25,200

The cost of heat exchangers is determined based on the heat transfer area as described in Eq. (2.16) [43]. Thus, the purchasing cost of the heat exchanger is defined by CAPCOST based on the heat exchanger area.

$$A_{HE} = \frac{Q_f}{U \Delta T_m} \tag{2.16}$$

$$\Delta T_m = \frac{\Delta T_1 - \Delta T_2}{ln\left(\frac{\Delta T_1}{\Delta T_2}\right)} \tag{2.17}$$

where A_{HE} represents the heat exchanger area (m^2), Q_f is the thermal power provided (J s^{-1}), U is overall heat transfer coefficient (W m^{-2} K^{-1}), and ΔT_m represents the logarithmic-mean temperature difference, the temperature difference between the inlet (ΔT_1) and outlet streams (ΔT_2) across the heat exchanger.

3.1.3. Pump cost

A pump is used to circulate the feed stream to the PV membrane module and to circulate cooling water. The power of the pump (E_p) is estimated as follows [44]:

$$E_p = q\, \rho\, g\, h \tag{2.18}$$

where E_p represents the power (Watt), q is the flow rate (m^3 s^{-1}), ρ is the liquid density (kg m^{-3}), g is the gravity acceleration (9.81 m s^{-2}) and h is the pump head (m). The purchasing cost of the pumps was estimated by CAPCOST based on the power requirement with 80% efficiency [20].

3.1.4. Vacuum pump cost

A vacuum pump is used to remove the permeate in the form of vapor. The power consumption of a vacuum pump (E_v) is estimated with Eq. (2.19). The equation is based on the principle of adiabatic vapor expansion and contraction [45].

$$E_v = \frac{m_c\, R\, T_p}{MW\, \varepsilon_p} \frac{\varphi}{\varphi - 1}\left[\left(\frac{P_{out}}{P_{in}}\right)^{\frac{\varphi-1}{\varphi}} - 1\right] \tag{2.19}$$

where m_c presents the mass flow rate of the non-condensable (air and CO_2 in g s^{-1}), ε_p is the efficiency of vacuum pump (80%), R is the universal gas constant (8.314 J mol^{-1} K^{-1}), T_p is the temperature in permeate side, MW is the molecular weight (air and CO_2, 43.36 g mol^{-1}), P_{out} is the exit pressure of the vacuum pump (atmospheric pressure, 1013.25 mbar), P_{in} is the vacuum pump inlet pressure, and φ is the adiabatic expansion coefficient. The adiabatic expansion coefficient (φ) is defined as [45]:

$$\varphi = \frac{C_{cp}}{C_{cv}} = \frac{C_{cp}}{C_{cp} - R_{air}} \tag{2.20}$$

where C_{cp} and C_{cv} are the heat capacity of air, at constant pressure (1 kJ kg^{-1}) and constant volume (0.718 kJ kg^{-1}), respectively, hence φ is 1.4, while R_{air} is the gas constant for air (0.287 kJ kg^{-1} K^{-1}).

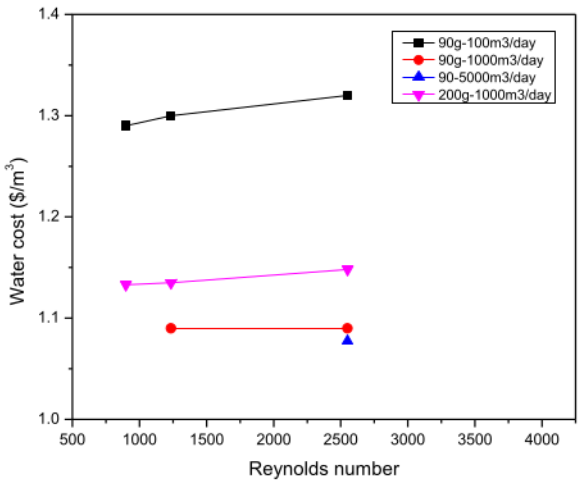

Fig. 4.1. The water cost at different Reynolds numbers (single module at different plan capacities and feed concentrations).

The purchasing cost of the vacuum pump is estimated based on the required capacity, the cost of the vacuum pump was reported in the literature [46] as shown in Table 2.2.

3.2. Sensitivity analysis

The economic model was used to estimate the water cost in the pervaporation desalination process. Model output is based on the capital cost plus operating and maintenance cost. There are some assumptions used to determine those costs. The sensitivity analysis was used to explore and calculate the impact of possible changes in input data on predicted model outputs. The sensitivity analysis is used to illustrate the water cost of alternative assumptions.

4. Results and discussion

4.1. Effect of different plant capacities and feed concentrations on the water production cost of pervaporation desalination

Fig. 4.1 presents the water production cost for different scenarios (see Fig. 2.2) at Reynolds numbers ranging from 898.27 to 2500. At the same Reynolds number, increasing the size (diameter) of the membrane in the PV system will decrease the velocity. The results showed that the same Reynolds number of 898.27 could not be set for capacity above

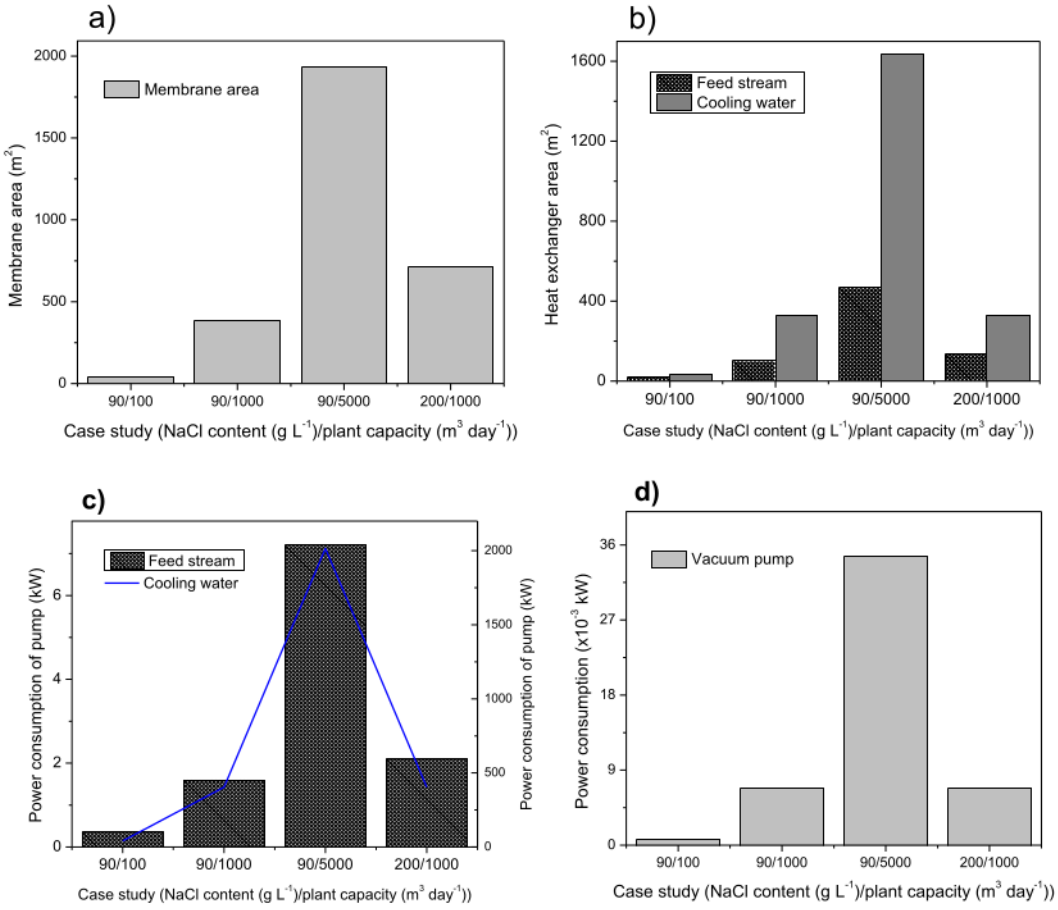

Fig. 4.2. The membrane area (a) and heat exchanger area (b) required; power consumption of pump (c) and vacuum pump (d) at different plan capacities and feed concentrations (single module).

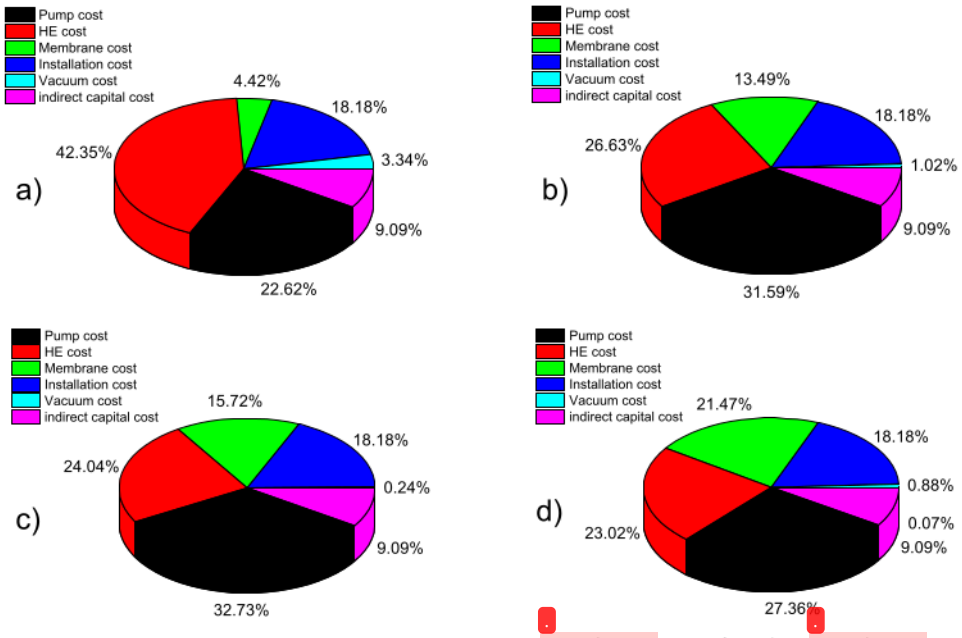

Fig. 4.3. Distribution of capital cost in different feed concentration and plant capacity: (a) 90 g L^{-1} of NaCl – 100 m^3 day^{-1}, (b) 90 g L^{-1} of NaCl – 1000 m^3 day^{-1}, (c) 90 g L^{-1} of NaCl – 5000 m^3 day^{-1}, (d) 200 g L^{-1} – 1000 m^3 day^{-1} (single module).

1000 m^3 day^{-1} at a feed concentration of 90 g L^{-1} because the feed flow rate was lower than the water production or permeate. Hence the feed flow rates were increased by enhancing the Reynolds number at minimum 1235 and 2550 for capacity 1000 and 5000 m^3 day^{-1}, respectively. Fig. 4.1 describes that increasing the plant capacity decreases the water production cost per m^3 of produced water. The water production cost reduces from \$1.32/m^3 to \$1.077/m^3 when the plant capacity enlarges from a small size of 100 m^3 day^{-1} to a medium size of 5000 m^3 day^{-1}. Besides, at the same plant capacity, increasing the feed concentration increases the water production cost. The water cost increases from \$1.09/m^3 to 1.15 \$/m^3 when the feed concentration increases from 90 g L^{-1} to 200 g L^{-1}. The increase in water cost due to the increment of feed concentration yields a decrease in water flux. The water flux decreased by 45.6% when the feed concentration increased from 90 g L^{-1} to 200 g L^{-1}, hence more membrane surface area was required to fulfill the plant capacity which resulted in an increased membrane cost.

To complete the economic study, the details of the calculation of the required membrane area, heat exchanger area, the power consumptions of the pump, and the vacuum pump for four scenarios are presented in supporting information (see supporting information in tables SI.1, SI.2. SI.3, SI.4., and SI.5). The results are summarized in Fig. 4.2.

Fig. 4.2a and b show that the membrane and heat exchanger area increases with the capacity and with feed concentration. The membrane area increases by 83.7% when the feed concentration increases from 90 to 200 g L^{-1}, while the total heat exchanger area increases by 8.4%. An increment in feed concentration results in a larger membrane and heat exchanger area because the water flux decreases when the feed concentration increases. Thus, additional equipment such as membrane units and heat exchangers may be needed to produce fresh water with a specified plant capacity. As presented in Fig. 4.2b, the heat exchanger area for circulating the cooling water takes a higher requirement than the feed stream, hence other technologies or methods to condense the permeate could be explored and investigated to reduce the water cost in the pervaporation desalination system. Fig. 4.2c and d show that increasing the plant capacity leads to a rise in power consumption of the pump and vacuum pump. However, an increment of feed concentration does not enhance the power consumption of the vacuum pump and pump for cooling water, nevertheless, the power consumption of the feed circulation pump increases by 31.3% when the feed concentration increases from 90 to 200 g L^{-1}. The power consumption of the feed circulation pump increases with the feed concentration because a higher feed concentration gives a lower water flux. Then, the membrane area is to be enlarged to produce the same plant capacity which results in more feed water to be processed.

4.2. Cost analysis

The estimated water cost for the PV membrane-based system is driven by capital costs and operating costs. Fig. 4.3 shows the distribution of capital cost at different feed concentrations and plant capacities. The cost of the membrane and the circulation pump increase along with the increment of plant capacity. In this study, the feed flow rate for all scenarios was targeted at laminar conditions. When the size (diameter) in the system is enlarged but the PV system uses the same Reynolds number, then the velocity or flow rate decreases. Hence, the heat exchanger cost decreases with the enhancement of plant capacity.

4.3. Effect of different configurations on the water cost of pervaporation desalination

The effect of different configurations on the water cost for pervaporation desalination was investigated with the single module, parallel and, series configuration. A plant capacity of 5000 m^3 day^{-1} at a feed stream of 90 g L^{-1} NaCl was used for the case study. Fig. 4.4 presents the configurations of pervaporation desalination that are studied.

The economic calculations of the pervaporation desalination process for three configurations are presented in Table 4.1.

From Table 4.1 can be seen that the water production cost increases when the configuration changes to parallel and series due to the additional equipment cost. The increment of equipment cost is due to the additional heat exchanger for a series and parallel configuration, and the additional pump in the series configuration, which leads to an increase

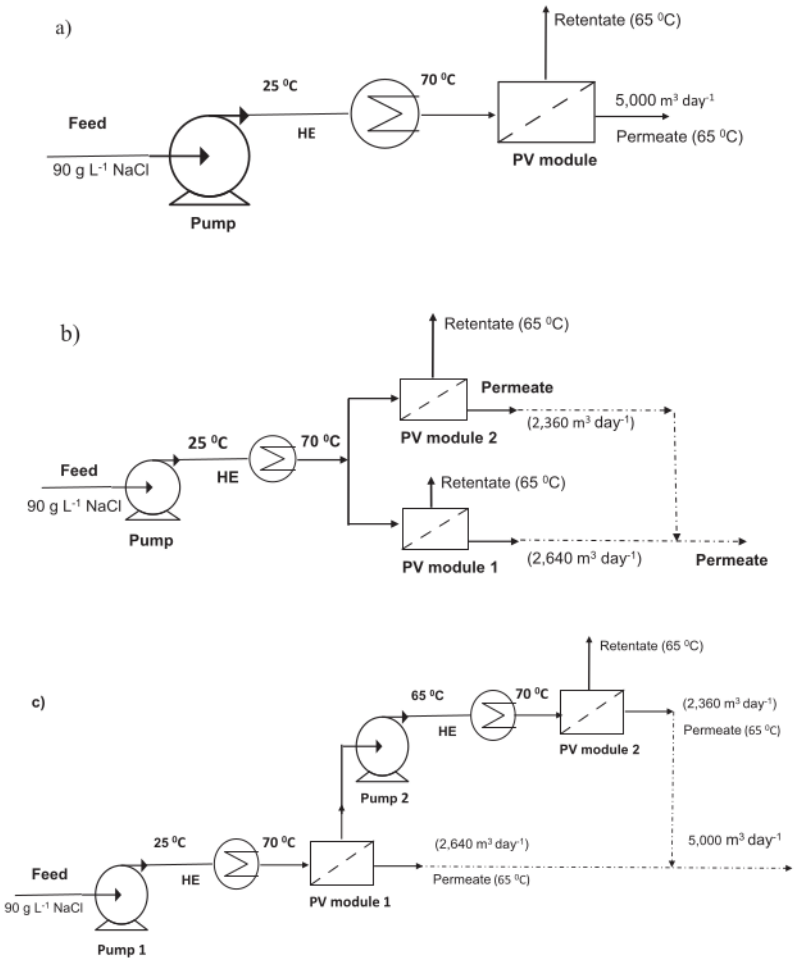

Fig. 4.4. Illustration of the configuration of pervaporation desalination for plant capacity of 5000 m^3 day^{-1} at feed stream of 90 g L^{-1} NaCl: a) Single membrane module, b) parallel with two membrane modules, and c) series with two membrane modules.

of the equipment cost. Thus, it influences the capital cost.

Table 4.1 highlights that the water production cost of a series configuration is lower than that of a parallel configuration. This is because the series configuration utilizes the hot retentate as a feed stream for the next stage, which reduces the surface area of the heat exchanger. As a consequence, the cost of the heat exchanger is reduced.

4.4. Process energy performance

Thermal energy is the energy to heat the feed stream to reach the operating temperature of 70 °C. The thermal energy requirement for different configurations is presented in Table 4.2.

Table 4.2 indicates that the thermal energy requirement of a series configuration is lower than for the single and parallel configuration. This is because the series configuration uses hot retentate as the feed stream for the next stage, which needs a low thermal energy compared to the previous stage. As shown in Table 4.2, the thermal energy of the series configuration is about 40.7 kWh/m^3. Wang et al. reported that thermal energy for a full-scale system of pervaporation desalination was 52.7 kWh/m^3 [31]. However, Xie et al. stated that for laboratory-scale pervaporation desalination, the thermal energy of 2.3 kWh/m^3 was desired to heat and maintain the feed stream at 65 °C [20]. In this study, we estimated the water cost using waste heat as the scenario. However, the water cost will increase proportionally when thermal energy is purchased.

4.5. Sensitivity analysis of the water cost

There were various uncertain parameters in the economic analysis. As shown in Fig. 4.3, variables such as the cost of a heat exchanger, the pump, and the membrane considerably affect the water production cost. Therefore, a sensitivity analysis was carried out to explore the changes in the water cost due to changes in each parameter or variable. In this case, the single module configuration as illustrated in Fig. 4.4a was explored as an example. The scenarios of the changing variables were investigated and presented in Table 4.3. The effect of variables changing on the water cost is presented in the supporting information in table SI.6 and summarized in Fig. 4.3.

Fig. 4.5 suggests that the variation of pump head and maintenance cost (O&M cost) has a significant effect on the water cost. The pump cost is the most influential on the water cost. The water cost decreases from 1.077 to 0.6 $/$m^3$ when the pump head reduces from 10 to 5 m. As shown in Fig. 4.3, the vacuum cost is contributing significantly to the water cost as it is around 30%.

Table 4.1
The water cost at different configurations of pervaporation desalination for plant capacity of 5000 m^3 day^{-1} with 90 g L^{-1} of NaCl in the feed stream. The significance of bold and data enclosed in a box are to make it easier for the reader which important variables determine the water cost for different configurations.

Description	The water cost at different membrane module configurations ($)		
	Single module	Parallel with two membrane modules	Series with two membrane modules
Pump cost	**564,910**	**566,200**	**572,860**
Vacuum cost	50,400	50,400	50,400
HE cost	**415,000**	**463,900**	**420,200**
Membrane cost	271,317.8	271,317.8	271,317.8
Total equipment	**325,406.9**	**1,351,817.8**	**1,314,777.8**
Installation cost	564,910	337,954.4	328,694.4
Indirect capital cost	162,703.5	168,977.2	164,347.2
Annual capital cost	**143,613.9**	**149,151.6**	**145,064.8**
Annual operating maintenance cost	1,626,751.1	1,653,418.2	165,3418.2
Annual electricity cost	**1,436,160.1**	**1,462,827.1**	**1,462,827.1**
Annual labor cost	82125	82,125	82,125
Annual membrane replacement cost	54,263.5	54,263.5	54,263.5
Annual maintenance cost	54,202.5	54,202.5	54,202.5
Total annual cost	1,770,365.1	1,802,569.8	1,798,483
Unit cost ($/m³)	**1.077**	**1.097**	**1.095**

Table 4.2
The thermal energy requirement at different configurations at plant capacity of 5000 m^3 day^{-1} with 90 g L^{-1} of NaCl in the feed stream.

Configuration	The energy requirement (Watt)	Total energy requirement (Watt)	Thermal energy requirement (kWh/m^3)
PV with single configuration	$Qf = 1.06 \times 10^7$	1.06×10^7	50.7
PV with series configuration with two modules	$Qf_1 = 7.67 \times 10^6$ $Qf_2 = 8.06 \times 10^5$	8.48×10^6	40.7
PV with parallel configuration with two modules	$Qf_1 = 5.57 \times 10^6$ $Qf_2 = 4.97 \times 10^6$	1.05×10^7	50.6

In addition to the variables mentioned in Fig. 4.5, variables such as the amount of water condensed by cooling and the water flux changes when the membrane is scaled up are also investigated and presented in Fig. 4.6. Fig. 4.6a shows that the water cost increases from 1.077 $/$m^3$ to 1.19 $/$m^3$ and 1.34 $/$m^3$ when the condensation of the permeate decreases from 100% to 90% and 80%, respectively. Fig. 4.6b describes that the water cost increases from 1.077 $/$m^3$ to 1.094 $/$m^3$ and 1.12 $/$m^3$ when the water flux decreased by 30% and 50%, respectively.

In this study, the temperature of the permeate was assumed of 35 °C. Fig. 4.7 illustrates the water cost when the permeate is changed to 30 °C and 27 °C. From Fig. 4.7 can be seen that the water cost change is not significant. The water cost increases from 1.077 $/$m^3$ to 1.084 $/$m^3$ and 1.094 $/$m^3$ when the temperature of permeate decreases from 35 °C to 30 °C and 27 °C, respectively.

Table 4.3
Variables used to investigate the water cost changes.

No.	Variable	Description
1.	Overall heat transfer coefficient (U) for heating.	The values: 15, 30, 50, and 70 (W m^{-2} K^{-1}).
2.	Overall heat transfer coefficient (U) for cooling.	The values: 1000, 2000, 3000 and 4000 (W m^{-2} K^{-1}).
3.	Membrane cost	The membrane cost decreases: 10%, 30%, and 50% per m^2. The membrane cost increases: 10%, 30%, and 50% per m^2.
4.	Pump	The pump height: 5, 7, and 10 m.
5.	Operating and maintenance cost	Operating and maintenance cost: 10%, 20%, 30%, and 40% from total operating cost used in this study.

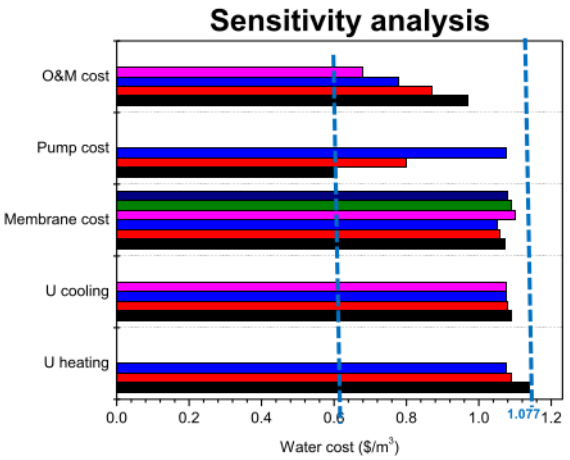

Fig. 4.5. Effect of variables changes on the water cost (single module).

Table 4.4 presents the water cost for different desalination processes such as multi-flash (MSF), multiple-effect evaporation (MEE), mechanical vapor compression (MVC), reverse osmosis (RO), and pervaporation (PV). The table shows that the water cost in this study is estimated ranging from 0.6 to 1.077 $/$m^3$ for a capacity of 5000 m^3 day^{-1}, which competes with other processes. Moreover, this study investigated the water cost for 90 g L^{-1} of NaCl as a feed stream while other processes use 35 g L^{-1} of NaCl in the feed stream.

4.6. Energy cost

In this study, the water cost was estimated by the free energy cost approach using blast furnace gas as waste heat from industry. However, if the scenario with purchased energy was also investigated; Table 4.5 shows the calculations.

Table 4.5 confirms that the water cost is projected around 1.077 $/$m^3$ when the PV desalination process is integrated by blast furnace gas as waste heat from industry. However, the water cost is stretching from 11.8 to 44.3 $/$m^3$ if using Coal and gas. PV desalination is one of the thermal-driven membrane processes, hence the energy cost significantly affects the water cost.

5. Conclusion

Energy is considered the most important parameter for PV desalination. Hence, this study was dedicated to an economic analysis of low-

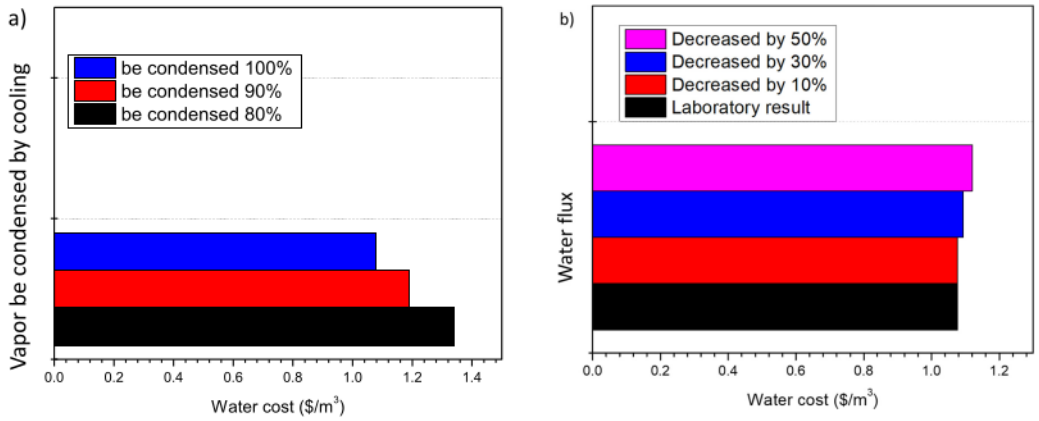

Fig. 4.6. Effect of a) vapor be condensed by cooling and b) decreasing water flux changes on the water cost (single module).

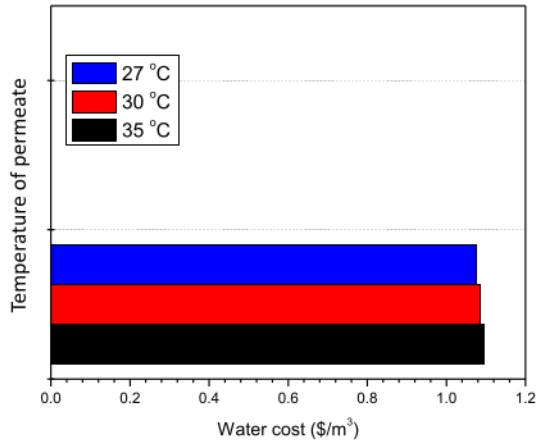

Fig. 4.7. Effect of decreasing permeate temperature on the water cost (single module).

Table 4.4
The water cost for different desalination processes [24,47,48].

Description	MSF	MEE	MVC	RO	PV
Typical average capacity (m^3 day^{-1})	25,000	10,000	3000	6000	This study (5000) With free energy cost
Feed stream	Seawater −35 g L^{-1} NaCl	Seawater −35 g L^{-1} NaCl	Seawater −35 g L^{-1} NaCl	Seawater −35 g L^{-1} NaCl	90 g L^{-1} NaCl
Water cost ($/m³)	**1.1**	**0.8**	**0.7**	**0.7**	**0.6–1.077**

The significance of bold is to make it easier for the reader to focus on the comparison of water cost for different desalination technolgies.

grade waste heat-driven PV desalination for producing fresh water from a hypersaline feed water source. The study indicated that the heat exchanger cost and pump cost especially for the cooling system was dominant in the PV desalination plant. Increasing the plant capacity decreased the water production cost, however when the feed stream concentration increased from 90 g L^{-1} to 200 g L^{-1} of NaCl (122.2%) at a plant capacity of 1000 m^3 day^{-1}, the water production cost increased.

Table 4.5
The water cost at different energy costs (this study).

Energy resource	Energy cost ($/MWh)	Water cost ($/m³)
Waste heat-blast furnace gas (this study)	Free	1.077
Conventional-coal	62–157 [49]	18.4–44.3
Conventional-gas	38–75 [49]	11.8–22

This increase is because an increasing NaCl concentration in the feed stream resulted in a decreasing water flux so that a larger membrane surface area was required to keep the plant capacity at the same level. Consequently, the capital cost increased. Comparing three configurations, i.e., single module, series with two modules, and parallel with two modules at a plant capacity of 5000 m^3 day^{-1} with 90 g L^{-1} NaCl in the feed stream, the water production cost of a single module is the lowest. This is because a series and parallel configuration require additional equipment, i.e., heat exchanger and pump, which gives an increased capital cost so that the water cost is higher. However, in energy performance, the series configuration gave the lowest thermal energy compared to the single and parallel configuration, because the series configuration employs the hot retentate as feed for the next stage, hence the thermal energy could be reduced. In this study, the proportion of pump and operating and maintenance costs towards the overall cost of pervaporation was substantial. The pump for circulating cooling water to condense the permeate is dominant on the pump cost. Therefore, it is necessary to investigate other cooling processes that can reduce water production costs, so that pervaporation becomes more attractive for desalination of hypersaline water application.

Declaration of competing interest

The authors declare that they have no known competing financial interests or personal relationships that could have appeared to influence the work reported in this paper.

Acknowledgment

This work was supported by the promoter, Prof.dr.ir. Bart van der Bruggen. We thank Mohammed Noorul Hussain for the fruitful discussions (KU Leuven).

Appendix A. Supplementary data

Supplementary data to this article can be found online at https://doi.org/10.1016/j.desal.2021.115538.

References

[1] E. Jones, M. Qadir, M.T.H. van Vliet, V. Smakhtin, S.Mu Kang, The state of desalination and brine production: a global outlook, Sci. Total Environ. 657 (December 2018) (2019) 1343–1356.

[2] A. Panagopoulos, K.J. Haralambous, M. Loizidou, Desalination brine disposal methods and treatment technologies - a review, Sci. Total Environ. 693 (2019).

[3] C. Boo, R.K. Winton, K.M. Conway, N.Y. Yip, Membrane-less and non-evaporative desalination of hypersaline brines by temperature swing solvent extraction, Environ. Sci. Technol. Lett. 6 (6) (2019) 359–364.

[4] T.M. Zewdie, N.G. Habtu, A. Dutta, B. Van der Bruggen, Solar-assisted membrane technology for water purification: a review, J. Water Reuse Desalin. 11 (1) (Nov. 2020) 1–32.

[5] T. Tong, M. Elimelech, The global rise of zero liquid discharge for wastewater management: drivers, technologies, and future directions, Environ. Sci. Technol. 50 (13) (2016) 6846–6855.

[6] S.K. Patel, P.M. Biesheuvel, M. Elimelech, Energy consumption of brackish water desalination: identifying the sweet spots for electrodialysis and reverse osmosis, ACS EST Eng. 1 (5) (2021) 851–864, https://doi.org/10.1021/acsestengg.0c00192.

[7] Q. Wang, N. Li, B. Bolto, M. Hoang, Z. Xie, Desalination by pervaporation: a review, Desalination 387 (2016) 46–60.

[8] Y. Wen, J. Yuan, X. Ma, S. Wang, Y. Liu, Polymeric nanocomposite membranes for water treatment: a review, Environ. Chem. Lett. 17 (4) (2019) 1539–1551.

[9] E. Halakoo, X. Feng, Layer-by-layer assembly of polyethyleneimine/graphene oxide membranes for desalination of high-salinity water via pervaporation, Sep. Purif. Technol. 234 (May) (2020) 116077, 2019.

[10] Y.L. Xue, J. Huang, C.H. Lau, B. Cao, P. Li, Tailoring the molecular structure of crosslinked polymers for pervaporation desalination, Nat. Commun. 11 (1) (2020).

[11] H. Zeng, et al., Hydrophilic SPEEK/PES composite membrane for pervaporation desalination, Sep. Purif. Technol. 250 (2020), 117265.

[12] A. Selim, et al., Preparation and characterization of PVA/GA/Laponite membranes to enhance pervaporation desalination performance, Sep. Purif. Technol. 221 (2019) 201–210.

[13] I. Prihatiningtyas, Y. Hartanto, B. Van der Bruggen, Ultra-high flux alkali-treated cellulose triacetate/cellulose nanocrystal nanocomposite membrane for pervaporation desalination, Chem. Eng. Sci. 231 (2021), 116276.

[14] J. Sun, X. Qian, Z. Wang, F. Zeng, H. Bai, N. Li, Tailoring the microstructure of poly (vinyl alcohol)-intercalated graphene oxide membranes for enhanced desalination performance of high-salinity water by pervaporation, J. Membr. Sci. 599 (2020), 117838.

[15] I. Prihatiningtyas, G.A. Gebreslase, B. Van der Bruggen, Incorporation of Al2O3 into cellulose triacetate membranes to enhance the performance of pervaporation for desalination of hypersaline solutions, Desalination 474 (2020), 114198.

[16] M.S. El-Bourawi, Z. Ding, R. Ma, M. Khayet, A framework for better understanding membrane distillation separation process, J. Membr. Sci. 285 (1) (2006) 4–29.

[17] Z. Xie, D. Ng, M. Hoang, T. Duong, S. Gray, Separation of aqueous salt solution by pervaporation through hybrid organic-inorganic membrane: effect of operating conditions, Desalination 273 (1) (2011) 220–225.

[18] D. Wu, A. Gao, H. Zhao, X. Feng, Pervaporative desalination of high-salinity water, Chem. Eng. Res. Des. 136 (2018) 154–164.

[19] R. Zhang, X. Xu, B. Cao, P. Li, Fabrication of high-performance PVA/PAN composite pervaporation membranes crosslinked by PMDA for wastewater desalination, Pet. Sci. 15 (1) (2018) 146–156.

[20] Z. Xie, D. Ng, M. Hoang, J. Zhang, S. Gray, Study of hybrid PVA/MA/TEOS pervaporation membrane and evaluation of energy requirement for desalination by pervaporation, Int. J. Environ. Res. Public Health 15 (9) (2018).

[21] T. Mezher, H. Fath, Z. Abbas, A. Khaled, Techno-economic assessment and environmental impacts of desalination technologies, Desalination 266 (1–3) (2011) 263–273.

[22] B. Van der Bruggen, Desalination by distillation and by reverse osmosis — trends towards the future, Membr. Technol. 2003 (2) (2003) 6–9.

[23] N.M. Wade, Distillation plant development and cost update, Desalination 136 (1) (2001) 3–12.

[24] G. Fiorenza, V.K. Sharma, G. Braccio, Techno-economic evaluation of a solar powered water desalination plant, Energy Convers. Manag. 44 (14) (2003) 2217–2240.

[25] C. Fritzmann, J. Löwenberg, T. Wintgens, T. Melin, State-of-the-art of reverse osmosis desalination, Desalination 216 (1) (2007) 1–76.

[26] S. Al-Obaidani, E. Curcio, F. Macedonio, G. Di Profio, H. Al-Hinai, E. Drioli, Potential of membrane distillation in seawater desalination: thermal efficiency, sensitivity study and cost estimation, J. Membr. Sci. 323 (1) (2008) 85–98.

[27] U.K. Kesieme, N. Milne, H. Aral, C.Y. Cheng, M. Duke, Economic analysis of desalination technologies in the context of carbon pricing, and opportunities for membrane distillation, Desalination 323 (2013) 66–74.

[28] S. Tavakkoli, O.R. Lokare, R.D. Vidic, V. Khanna, A techno-economic assessment of membrane distillation for treatment of Marcellus shale produced water, Desalination 416 (February) (2017) 24–34.

[29] L. Gao, S. Yoshikawa, Y. Iseri, S. Fujimori, S. Kanae, An economic assessment of the global potential for seawater desalination to 2050, Water (Switzerland) 9 (10) (2017) 1–19.

[30] United States Department of Energy, Chapter 6: innovating clean energy technologies in advanced manufacturing | process intensification technology assessment, in: Quadrenn. Technol. Rev. 2015, 2015, pp. 1–28.

[31] J. Wang, D. Tanuwidjaja, S. Bhattacharjee, A. Edalat, D. Jassby, E.M.V. Hoek, Produced water desalination via pervaporative distillation, Water (Switzerland) 12 (12) (2020).

[32] 26th ITTC Specialist Committee, Fresh water and seawater properties, Int. Towing Tank Conf. 5 (10) (2011) 1596–1599.

[33] F. Banat, N. Jwaied, Economic evaluation of desalination by small-scale autonomous solar-powered membrane distillation units, Desalination 220 (1) (2008) 566–573.

[34] M.C. Sparenberg, I. Ruiz Salmón, P. Luis, Economic evaluation of salt recovery from wastewater via membrane distillation-crystallization, Sep. Purif. Technol. 235 (September) (2020) 116075, 2019.

[35] H.M. Ettouney, H.T. El-Dessouky, R.S. Faibish, P.J. Gowin, Evaluating the economics of desalination, Chem. Eng. Prog. 98 (12) (2002) 32–39.

[36] F. Macedonio, E. Curcio, E. Drioli, Integrated membrane systems for seawater desalination: energetic and exergetic analysis, economic evaluation, experimental study, Desalination 203 (1–3) (2007) 260–276.

[37] W. Van Hecke, E. Joossen-Meyvis, H. Beckers, H. De Wever, Prospects & potential of biobutanol production integrated with organophilic pervaporation – A techno-economic assessment, Appl. Energy 228 (March) (2018) 437–449.

[38] A.M. Helal, A.M. El-Nashar, E. Al-Katheeri, S. Al-Malek, Optimal design of hybrid RO/MSF desalination plants part I: modeling and algorithms, Desalination 154 (1) (2003) 43–66.

[39] V. Karanikola, S.E. Moore, A. Deshmukh, R.G. Arnold, M. Elimelech, A.E. Sáez, Economic performance of membrane distillation configurations in optimal solar thermal desalination systems, Desalination 472 (July) (2019), 114164.

[40] N. Kuipers, et al., Techno-economic assessment of boiler feed water production by membrane distillation with reuse of thermal waste energy from cooling water, Desalin. Water Treat. 55 (13) (2015) 3506–3518.

[41] I.-. Noor, A. Martin, O. Dahl, Techno-economic system analysis of membrane distillation process for treatment of chemical mechanical planarization wastewater in nano-electronics industries, Sep. Purif. Technol. 248 (April) (2020), 117013.

[42] M.H. Sharqawy, S.M. Zubair, V.J.H. Lienhard, Thermophysical properties of seawater: A review of existing correlations and data, Desalin. Water Treat. 16 (1–3) (2010) 354–380.

[43] S.J.M. Cartaxo, F.A.N. Fernandes, Counterflow logarithmic mean temperature difference is actually the upper bound: a demonstration, Appl. Therm. Eng. 31 (6–7) (2011) 1172–1175.

[44] J. Yu, T. Zhang, J. Qian, Efficiency testing methods for centrifugal pumps, Electr. Mot. Prod. (2011) 125–172.

[45] Z. Xie, et al., Preliminary evaluation for vacuum membrane distillation (VMD) energy requirement, J. Membr. Sci. Res. 2 (4) (2016) 207–213.

[46] H.P. Loh, J. Lyons, I.I.I.Charles W. White, Process Equipment Cost Estimation, Final Report, in: Other Inf. PBD 1 Jan 2002, no. January, p. Medium: ED; Size: 410 Kilobytes pages, 2002.

[47] N.M. Wade, Distillation of plant development and cost update, Desalination 136 (1–3) (2001) 3–12.

[48] O.J. Morin, Desalting plant cost update: 2000, in: Proceedings of the IDA World Congress on Desalination and Water Reuse, San Diego (USA) vol. III, 1999, pp. 341–359.

[49] Lazard, in: Lazard's Levelized Cost of Energy Analysis Version 13.0 vol. 11, Lazard Freres Co, 2020, pp. 1–21, no. November.

Techno-economic assessment of pervaporation desalination of hypersaline water

ORIGINALITY REPORT

2%	3%	5%	0%
SIMILARITY INDEX	INTERNET SOURCES	PUBLICATIONS	STUDENT PAPERS

MATCH ALL SOURCES (ONLY SELECTED SOURCE PRINTED)

4%

★ Indah Prihatiningtyas, Yi Li, Yusak Hartanto, Anja Vananroye, Nico Coenen, Bart Van der Bruggen. "Effect of solvent on the morphology and performance of cellulose triacetate membrane/cellulose nanocrystal nanocomposite pervaporation desalination membranes", Chemical Engineering Journal, 2020

Publication

Exclude quotes	On	Exclude matches	< 2%
Exclude bibliography	On		